*American Mineralogist, Volume 80, pages 823–832, 1995*

# Oscillatory zoning in meteoritic forsterite

**Ian M. Steele**
Department of Geophysical Sciences, University of Chicago, 5734 South Ellis Avenue, Chicago, Illinois 60637, U.S.A.

## Abstract

Some isolated forsterite grains in Allende (C3V) and ALHA 76004 (LL3) show oscillatory zoning when viewed with cathodoluminescence. Concentration profiles for these grains show that the oscillations correspond to cyclic variations in Al and Ti and, by inference with known correlations, V and Sc. Other elements, including Mg, Fe, Ca, and Cr, show only monotonic changes across the oscillatory-zoned area. Under reducing conditions assumed present during forsterite growth, the varying elements should be trivalent or higher in charge, whereas the Mg-Fe-Ca-Cr group would be divalent. Substitution into the olivine structure is considered to be two trivalent elements, dominated by Al, for Mg + Si, which represents a small substitution of the spinel component into forsterite. This same type of substitution is proposed for similar terrestrial oscillatory-zoned olivines in which no Fe or Mg variation is found.

By analogy with terrestrial and lunar oscillatory-zoned minerals, crystallization of the forsterite from a liquid is probable. Currently, no such source material is known, although crystallization of porphyritic chondrules may produce grains of equivalent size with zoning. Although no oscillatory-zoned forsterite has been observed in chondrules, their recognition may be confirmation of the source of isolated forsterite grains; alternatively, the source of these forsterite grains has not yet been recognized.

## Introduction

Chemical zoning of Mg and Fe is a conspicuous feature of most olivine grains that have crystallized from a magma. In normal mafic systems the earliest crystallizing olivine (the core) tends to be Mg rich relative to later olivine (the rim). In a recognized variation of this simple trend, the later growing olivine is more Mg rich than the olivine nearer the core. This is termed reversed zoning. Examples of interruptions or possible reversals of fine-scale zoning have been described (e.g., Van Kooten and Buseck, 1978) in which a normal zoning trend in a terrestrial olivine phenocryst is briefly interrupted by a slight increase in Mg and then a return to normal Fe enrichment. In this case the reversals are repeated several times from core to rim and superimposed on an overall normal zoning trend.

Minor-element zoning in olivine is seldom documented as carefully as Mg-Fe zoning. Of the three elements commonly determined using microprobe techniques, Mn is highly correlated with Fe, Ni is anticorrelated with Fe, and Ca concentration is variable and thought to reflect external parameters, including pressure, temperature, composition of surrounding magma (Watson, 1979), and growth rate. Few systematic data are available for P, Cr, Al, and Ti, which occur at $< 0.0\times$ levels in most olivines but at much higher levels in some meteoritic and lunar olivine in which V and Sc may also be detected with careful electron probe measurements (Steele, 1989).

Cathodoluminescence (CL) of terrestrial olivine is observed only for the most Mg-rich samples (FeO less than ~2 wt%), which excludes most common magmatic olivines in which Fe quenches the CL. Nearly pure forsterite is relatively common in some meteorites, and with FeO less than about 2 wt%, CL is readily observed under routine electron probe operating conditions. There is a positive correlation of Al, Ti, Ca, Sc, and V with increasing CL intensity and an inverse correlation in intensity with Fe, Cr, and Mn (Steele, 1986a). When imaging techniques are used, CL intensity reveals gross zoning patterns in forsterite (Steele, 1986a, 1986b). More sensitive CL detection methods have revealed additional features that correspond to oscillatory zoning (Steele, 1990). This is apparently the first description of oscillatory zoning in meteoritic olivine and only the second description of this zoning in any olivine, the first being for olivines from several terrestrial lava flows (Clark et al., 1986). The origin of meteoritic forsterite is controversial (Olsen and Grossman, 1978; McSween, 1977; Jones, 1992), but observations of features such as these zoning patterns should provide indications of both olivine formation and early events in the solar system.

## Experimental methods

Cathodoluminescence imaging of meteorites was performed on polished thin sections of Allende (C3V) and ALHA 76004 (LL3) using a Cameca SX-50 electron microprobe. The port for microscopic viewing was replaced with a photomultiplier with an S20R (blue sensitive) pho-

0003–004X/95/0708–0823$02.00

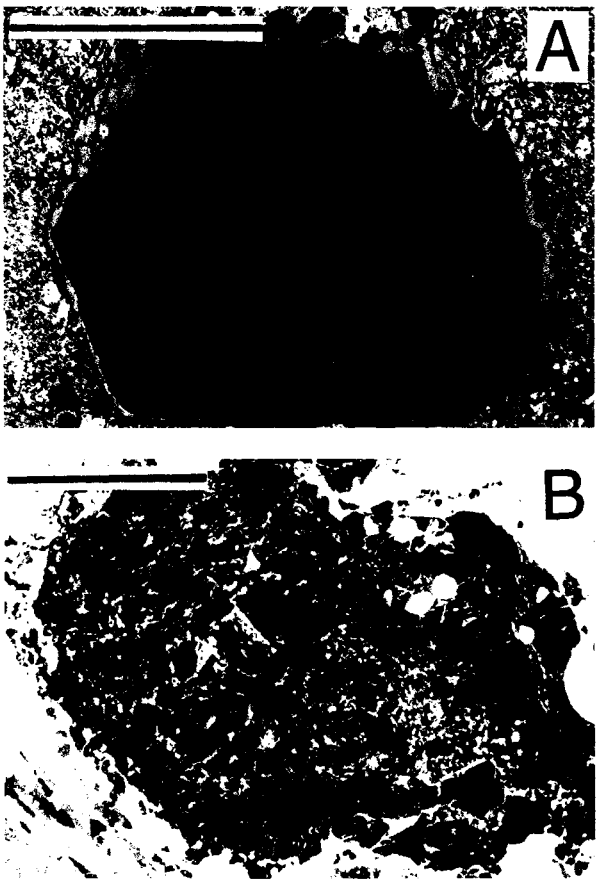


Fig. 1 (**A**) Mixed BSE-CL image of Allende forsterite. The central gray region is due to CL from nearly pure forsterite, whereas the darker rim represents forsterite with higher Fe than the central area. The grain is subhedral with crystal faces apparent on the bottom, left, and right. (**B**) BSE image of an inclusion in ALHA 76004. The dark angular grains are forsterite and the light gray is matrix consisting of fine, elongate, diopsidic pyroxene crystals with interstitial glass interpreted as a quench texture. Tiny white areas and crack fillings are mostly gold from previous studies that could not be removed. Finer grained matrix surrounds both the Allende grain and 76004 inclusion. Scale bars = 200 $\mu$m.

tocathode. The multiplier output was directed to the normal secondary-electron detector electronics providing a scanning CL image on a CRT analogous to a SE or BSE image. This image was recorded on Polaroid film.

Digital CL images (Steele, 1992) and BSE images were obtained using beam scanning and integration of outputs from the BSE and photomultiplier CL detector after analogue-to-digital conversion. The image size was fixed at 512 × 512 with a pixel size of 1.0 $\mu$m. The advantage of the digital images is that they can be processed with image-processing software to enhance specific features. Original and enhanced images were photographed directly from the Macintosh monitor using ASA 100 black-and-white film and a telephoto lens to reduce distortion.

Elemental scans were made by setting the four wavelength dispersive spectrometers on peak for Al, Ti, Cr, and Fe for one traverse and Al, Sc, V, and Ca for a second parallel traverse offset by about 10 $\mu$m from the first. Beam scanning was used with 0.5 $\mu$m steps, a total of 100 steps, and a counting time of 540 s/step for the two traverses. Beam conditions were 100 nA incident current, 20 kV, focused beam, and PHA set to include pulse distributions from the peaks of interest. Backgrounds were obtained by setting spectrometers off peak, and reference intensities were obtained from standards. No matrix corrections were applied as relative intensities are sufficient to illustrate concentration changes as a function of CL intensity. Detection levels determined from counting statistics were <40 ppm by weight for all elements, although Sc was the only analyzed element near this detection limit.

## Occurrence of oscillatory zoning

Forsterite occurs in the Allende meteorite as 0.1–1 mm isolated euhedral grains, similarly sized anhedral single crystals, and components of multiphase chondrules and aggregates. Provided the FeO content is below about 2 wt%, these grains emit CL that can be observed visually in the electron microprobe optics or detected by a photomultiplier and displayed on a CRT. Many of these olivine grains are zoned from forsterite to more Fe-rich rims or include cracks containing Fe-rich olivine; these rims and cracks do not show CL because of their high Fe content. Figure 1A shows a scanning image of a subhedral forsterite grain using an electronically mixed BSE and CL signal. This image shows both the atomic number distribution (mainly Fe/Mg) and CL features. The central portion of the grain shows an even CL brightness, whereas the 30 $\mu$m rim and several cracks appear dark because of increased Fe content. An optical image of this same grain was illustrated previously in Steele et al. (1985).

Figure 1B illustrates a complex inclusion in an unequilibrated ordinary chondrite, ALHA 76004 (LL3) (Olsen et al., 1978; Mayeda et al., 1980). This meteorite is a very heterogeneous breccia consisting of chondrules, chondrule fragments, clasts of crystalline rocks, glass, and interstitial quenched glass (Olsen et al., 1978). The inclusion shown in Figure 1B consists of about 40% by area of angular, fractured forsterite grains concentrated near the inclusion center; 30% Mg-rich, Ca-poor pyroxene with forsterite concentrated near the inclusion edge; and 30% fine-grained matrix of diopsidic pyroxene and Ca- and Al-rich glass showing a typical quench texture with elongated pyroxene forming radiating clusters with interstitial glass. Several small Fe,Ni-Fe,FeS clusters are also present. The inclusion boundary is not circular, possibly suggesting that this is not a chondrule but rather a portion of a larger body. The scalloped outline is similar to many other glass-rich inclusions (e.g., Fig. 3 of Olsen et al., 1978). The fragments of forsterite show no indication of an original euhedral morphology, possibly indicating that the olivine did not crystallize in situ but rather may have

been a relic grain later surrounded by a liquid that partially crystallized to the pyroxene-glass assemblage. Although this inclusion may be interpreted as a chondrule, there is indication of a complex history, and the nongenetic term, inclusion, is used here.

Digital CL images of the grain shown in Figure 1A taken with a much higher gain (contrast) reveal faint linear features (Fig. 2A with an inset showing the central area magnified). Several features are clearly shown. The upper portion of the grain appears very bright in contrast to the lower portion, which has narrow horizontal and inclined bands. The contact between the upper and lower portions is generally sharp but with greater contrast across the boundary near the grain edges. The faint CL bands of the lower half change direction corresponding to the crystal faces (Fig. 1A). The inset shows greater detail within the horizontal bands, with six bright bands between the bright CL region at the top and the relatively wide dark band toward the bottom. The rows of dark dots result from previous electron probe analyses in which CL was destroyed by electron beam damage.

Because Figure 2A is a digital image, convolution filters can be used to extract specific information. For the image shown in Figure 2A, a gradient filter (Gonzalez and Wintz, 1987) was applied to enhance features that have a horizontal component. This operation produced the image shown in Figure 2B. The horizontal bands are clearly highlighted and weaker bands both near the bottom of the CL area and at angles to the horizontal bands are now recognized. All are parallel to the CL boundaries and the grain edges. This image clearly shows the six bands that were faintly shown in the Figure 2A inset and allows measurement of period with higher accuracy.

Similar bands revealed by cathodoluminescence have been seen in other olivine grains in C3 carbonaceous and unequilibrated ordinary chondrites. None are as extensive and in such a euhedral grain as shown in Figure 2. Another example, however, of a forsterite grain from the central portion of the inclusion in Figure 1B is shown in Figure 3A and 3B. The BSE image (Fig. 3A) shows a single crystal of forsterite with numerous fractures surrounded by the fine-grained matrix. A CL image of the same scene (Fig. 3B) clearly shows a series of near vertical bands on the left side of the grain similar to those of the previously described Allende grain. Although these bands are nearly parallel to the edge of the olivine grain, they are clearly truncated at high angles at both the top and bottom, probably because of fracturing.

These two examples illustrate features reminiscent of oscillatory zoning commonly seen in plagioclase feldspar and pyroxene with a polarizing microscope. Oscillatory zoning has also been recognized in terrestrial olivine, but more involved techniques (acid etching and Nomarski interference microscopy) must be used to see it (Clark et al., 1986). In all cases, parallel features are indicated with a periodicity of micrometers and an orientation reflecting crystal growth directions. For the present examples of meteoritic forsterite, these features are revealed by cathodoluminescence; they are not seen using standard microscopic techniques, and etching is impractical for such small and complex materials.

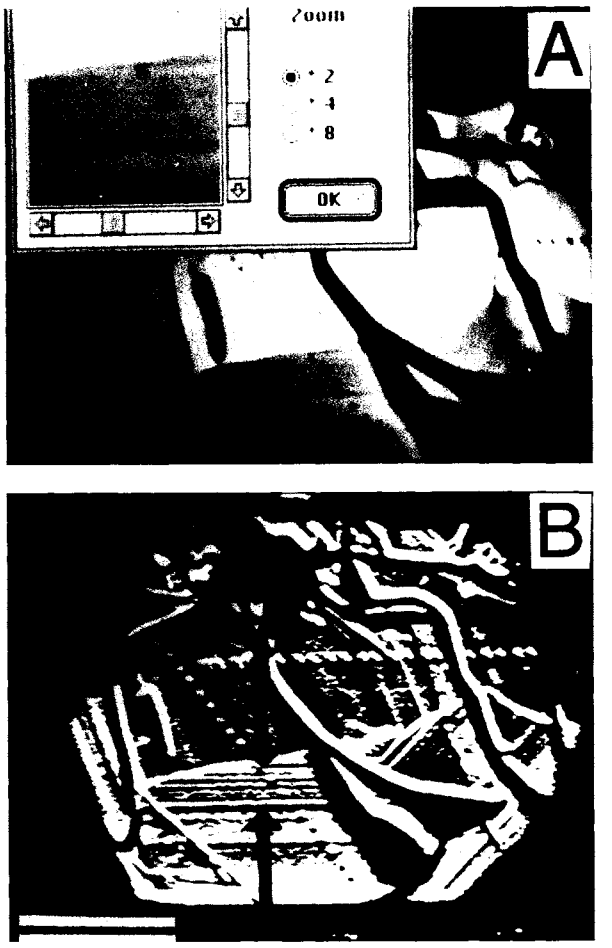


Fig. 2. (A) Digital CL image of Allende grain shown in Fig. 1A. Image was photographed from Macintosh computer screen. CL bands follow luminescence boundaries, which in turn are parallel to grain boundaries. The inset shows magnified view of lower center of forsterite grain. Rows of dots represent electron beam damage from previous analyses. (B) Processed image in which horizontal features are clearly enhanced. This image shows the six bands (between arrows) shown in the inset of A. Other straight CL bands, not apparent in A, are also clearly shown. Scale bar = 100 μm.

## Compositional variation and oscillatory zoning

### Allende forsterite

The regular variation in CL intensity most logically is correlated with compositional changes, although effecting elements may be at concentrations too low for variation to be detected. Alternatively, various types of defects not related to any element can cause different CL intensities. Using the electron microprobe with conditions set to optimize the minimum detection limit, step scans were made

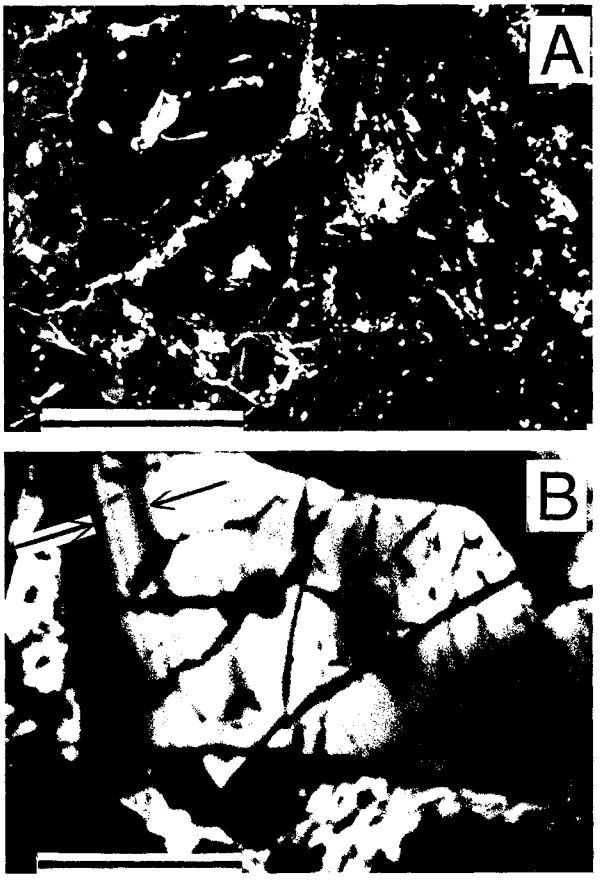


Fig. 3. (A) BSE image of forsterite grain within inclusion shown in Fig. 1B. Surrounding gray areas are a pyroxene-glass quench matrix; many small bright areas represent gold from previous conducting layer. (B) Same scene as in A but in CL. The left portion of the grain shows oscillatory zoning as near vertical straight bands. These bands intercept the grain boundaries at high angles, indicating that the crystal has been broken. The arrows at upper left show position of scan for which compositional data are illustrated in Figs. 7 and 8. Scale bars = 50 $\mu$m.

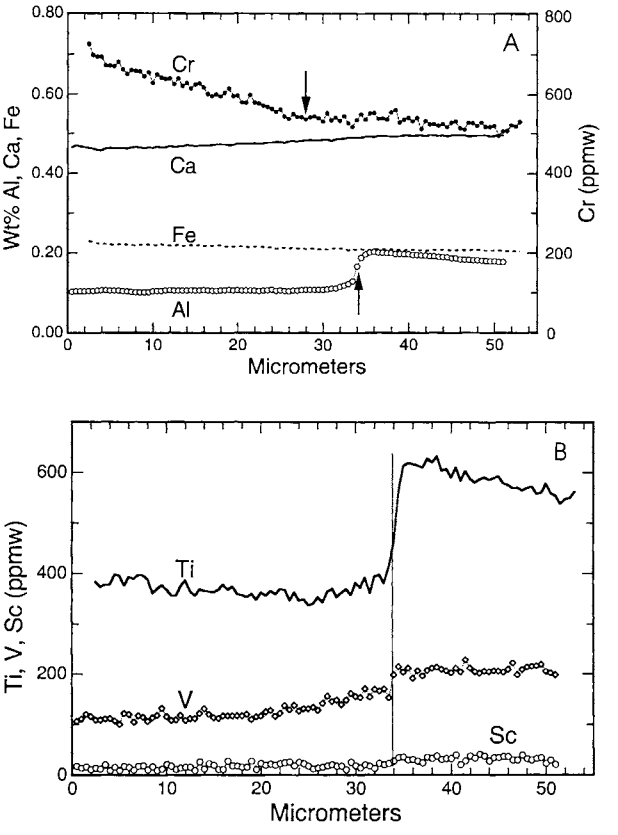


Fig. 4. (A) Concentration profiles for Al, Fe, Ca, and Cr extending from near lower arrow in Fig. 2B toward grain center, crossing the horizontal bands, and ending within bright CL region above top arrow in Fig. 2B. The step in Al marked at 34 $\mu$m marks the change from dull to bright CL at tip of the top arrow shown on Fig. 2B. Note that both Fe and Ca show no apparent change at this CL boundary, and the slight change in slope for Cr (arrow at 28 $\mu$m) does not correspond to the step in Al. (B) Concentration profiles for Ti, V, and Sc corresponding to same traverse shown in A. Both Ti and V show obvious steps at a position corresponding to that of Al. The profile for Sc shows a weak step at the same position when the total profile is considered in order to provide better statistics.

approximately perpendicular to both the fine and coarse CL features of Figure 2. The beginning position (=0 $\mu$m on all figures) is at the bottom arrow on Figure 2B, and the end of the scan is near the grain center within the bright CL area. Beam scanning (as opposed to stage scanning) was used to provide constant step size set at 0.5 $\mu$m realizing that the analyzed volume would be significantly greater. A total of seven elements were determined, and their variations are illustrated in Figures 4, 5, and 6.

Figure 4A illustrates Cr, Ca, Fe, and Al variation. It is obvious that the Al concentration changes abruptly at the bright-dull boundary, the high Al concentration being associated with the bright CL. In contrast, Ca and Fe show no change at this boundary, with Fe showing a weak increase and Ca a weak decrease from grain center toward grain edge. The increase in Fe is as expected for normal olivine zoning; the decrease in Ca is not indicative of any one process because there are many variables affecting its incorporation in the olivine structure. Cr shows a slight kink at a position that does not correspond to the CL boundary but rather is displaced about 6 $\mu$m toward the grain edge. Figure 4B illustrates the variation for three elements at low concentrations and not normally considered in an olivine analysis. Ti closely mimics Al with a step corresponding to the same position as seen for Al. A step in V is small but distinct, whereas the Sc data show this step only when visual averaging is made on either side of the known step position (vertical line). Expanded concentration scales are shown for Cr, Ca, and Fe in Figure 5. Careful examination reveals that the kink in the Al scan (at 34 $\mu$m, marked by vertical dashed line) also corresponds to a slight change in Fe and a more noticeable change in the Ca slope.

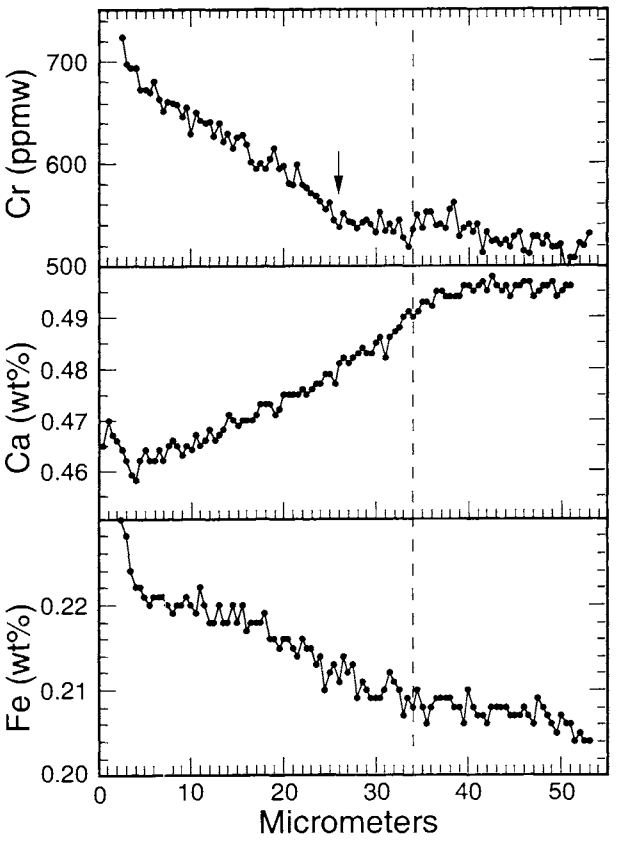


Fig. 5. Expanded scale for Cr, Ca, and Fe variation shown in Fig. 4A. Sharp CL boundary is marked by vertical dashed line and oscillatory-zoned portion of profile is to the left of dashed line. Both Ca and Fe show slight slope changes at the sharp CL boundary, whereas Cr shows a change at position marked by arrow. The concentrations of the three elements do not appear to reflect the presence of the oscillatory zoning.

The overall levels of trace and minor elements are similar to those recognized for forsterite from many extraterrestrial samples. Of the elements measurable with the electron probe, two groups are apparent: Fe, Ca, Cr, and Mn, and Al, Ti, V, and Sc. The inclusion of Mn in the Fe group is based on the high correlation of these two elements from other studies of similar forsterite. One obvious difference between these two groups is that the Fe group ions are divalent, whereas the Al group ions are trivalent. A qualification must be made in that with reducing conditions thought to be present in the solar nebula and on the Moon, Cr is predominantly divalent. A similar argument can be made for Ti and V, which are trivalent under reducing conditions.

The vertical scales in Figure 4A and 4B are not suitable for examining concentration variations in the portion of the traverse across the oscillatory zoning. Figure 6 shows a rescaled plot for Ti and Al, the data of which were collected in the same scan. A recognizable low Al area between 8 and 10 $\mu$m is apparent in the Al scan and is slightly displaced because the sharp CL boundary is at a small angle to the oscillatory-zoning lamellae. Also apparent are six peaks in one Al scan between the sharp CL boundary and the wide minimum at the 8–10 $\mu$m position. A comparison of the Ti and Al intensities shows several recognizable correlations. Although the error for Ti is large because of the low count rate, a set of lines is drawn that appears to connect high or low concentrations in the Ti and Al scans. In Figure 5 there are no recognizable regular variations in the Fe, Ca, or Cr scans corresponding to those seen for Al and Ti in Figure 6.

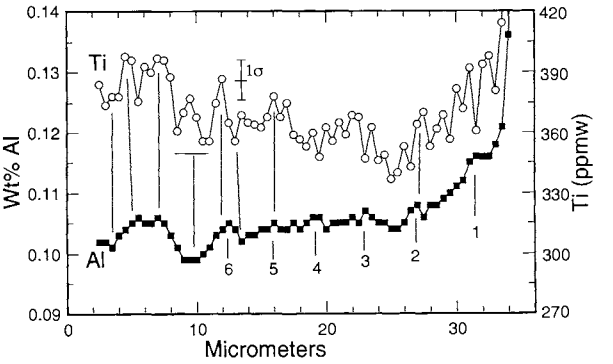


Fig. 6. Expanded scale for a portion of the Ti and Al profiles of Fig. 4A, which cross the six bands between arrows in Fig. 2B. The positions of these six bands, labeled 1–6, were measured from the inset of Fig. 2A and correspond closely to the maxima in the Ti and Al profiles. Although Ti data have a large error as noted by the error bar, several apparent matches between the two scans are indicated by vertical lines, suggesting a good correlation between Ti and Al.

### ALHA 76004 forsterite

A microprobe scan across the oscillatory zoning in the forsterite of 76004 shown in Figure 3 was made between the pictured arrows. Figure 7 shows the variation of Cr, Ca, and Fe. Trends similar to the Allende grain are seen, with Ca decreasing and Cr and Fe increasing from the grain interior toward the grain edge. There is no apparent correlation of CL intensity bands with these three elements, although the Cr profile appears to show a break in slope near the 14 $\mu$m position. Figure 8 illustrates the variation of Ti and two parallel scans for Al. The vertical lines indicate the positions of bright CL bands as measured from high magnification images. The two parallel Al scans are nearly identical in shape with peaks corresponding to the CL maxima. Likewise, the Ti profile shows peaks or shoulders at positions nearly identical to those in the Al profiles.

## Discussion

### Minor-element substitution in forsterite

The compositional data show a rather clear qualitative correlation between the CL intensity and the concentrations of Al, Ti, V, and Sc for the sharp, near-horizontal CL boundary shown on Figure 2A. The CL intensity of individual oscillatory zones correlates with Al and Ti as

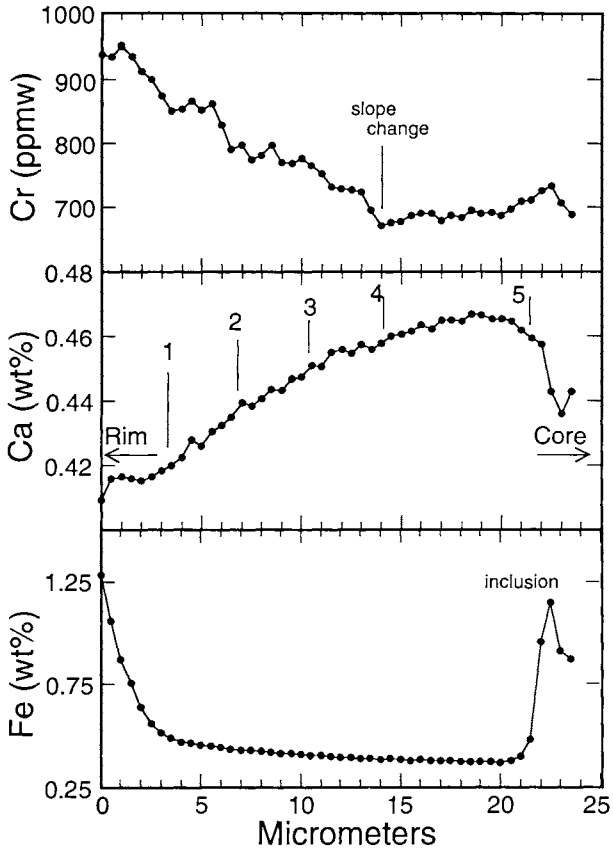


Fig. 7. Concentration profiles for Fe, Ca, and Cr across profile marked by arrows on upper left of Fig. 3B for 76004 forsterite. The grain rim at left shows normal enrichment in Fe and Cr and depletion in Ca relative to the core (right). The position of the bands owing to bright CL are labeled from 1 to 5, and these maxima in CL intensity are not reflected in the concentration profiles of the three elements. The Cr profile shows an apparent break in slope similar to that seen for the Allende forsterite in Fig. 5.

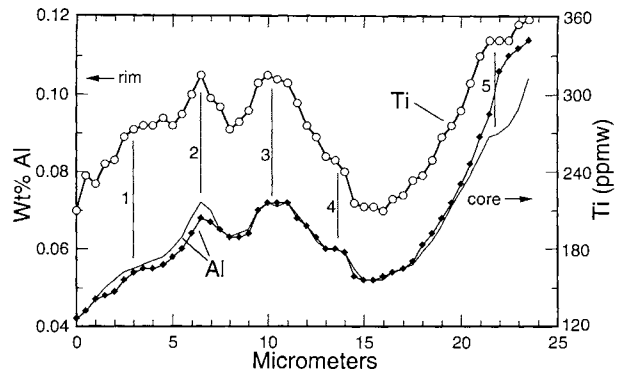


Fig. 8. The same profile as shown in Fig. 7 but for Al and Ti. These two elements are highly correlated, and the five maxima in CL intensity indicated by vertical lines closely match the maxima in Al and Ti seen as either distinct peaks or shoulders in their profiles.

shown in Figure 6 for Allende and in Figure 8 for 76004 olivine. A correlation between CL intensity and the concentration of V and Sc was previously documented for Allende olivine (Steele, 1986a), and by inference this correlation is extended to V and Sc along the profile of Figure 6 in the oscillatory-zoned region, although both elements are at too low a concentration to be measured accurately. There is a small inflection of Ca and Fe and none for Cr at the sharp horizontal CL boundary and no apparent fine-scale variation of Ca, Fe, or Cr corresponding to the CL bands. Although Mn was not determined, all previous studies on similar forsterite grains show an excellent positive correlation between Fe and Mn. These observations lead to the conclusion that as a group, Al, Ti, V, and Sc show a similar response to the conditions that cause the oscillatory zoning and compositional steps in these olivines. In contrast, the group of Fe, Cr, Ca, and Mn is not influenced by these conditions but rather shows a conventional monotonic change from core to rim, although Cr shows a change in slope.

These observations suggest that the causal factors affect one group of elements and not the other and that the controlling factors are common to each group of elements. The Al-Ti-V-Sc group of elements is incompatible (crystal-liquid distribution coefficients $\ll 1$) in the olivine structure under usual petrologic conditions, such as those found on the Earth and Moon. Of these four elements, Al and Sc are trivalent, but Ti can be either trivalent or quadravalent. Both oxidation states have been detected in lunar (Burns et al., 1973) and Allende ferromagnesian (Beckett and Grossman, 1986) phases and in oxide (Beckett et al., 1988) phases. Similar reducing conditions are expected during growth of the forsterite on the basis of the absence of Ni and the very low Fe content of the forsterite because both elements are presumably present as metal species and major $Ti^{3+}$ is expected. The oxidation state of V, except under the most oxidizing conditions on Earth ($V^{5+}$), is usually considered as trivalent. It is possible under very reducing conditions to obtain $V^{2+}$; however, for the conditions of crystallization for Allende fassaites, $V^{3+}$ is stable (Beckett and Grossman, 1986). Significant (percent level) substitutions of trivalent elements are possible in the presence of univalent Li as demonstrated in synthetic systems (Ito, 1977), but there is no indication that Li is present in these forsterite grains.

For the Fe-Cr-Mn-Ca group, the elements are all compatible in the olivine structure (crystal-liquid distribution coefficients near 1). Although Cr is usually considered to be trivalent, $Cr^{2+}$ can be present under reducing conditions. Evidence for this is by analogy with lunar mare olivine, the relatively high Cr content of which has been attributed to $Cr^{2+}$ (Scheetz and White, 1972) and experimentally measured by XANES (Sutton et al., 1993). The oxidation state of Cr in the forsterite showing oscillatory zoning is unknown, but it is reasonable to assume that it is similar to that of the Moon because of the absence of

Ni and the very low Fe content, both of which are consistent with very reducing conditions.

The absence of fine-scale compositional changes for Fe and Mg in oscillatory-zoned regions of terrestrial olivine of clearly magmatic origin (Clark et al., 1986) might correlate with variations in the minor trivalent ions that were not determined. In contrast, the observation of fine-scale variations in Fe, Mg, and Mn for other meteoritic olivine (Petaev and Brearley, 1994), which probably represents a metamorphosed magmatic olivine, suggests that different processes or conditions can form features not unlike that of oscillatory zoning. There were no measurements of other minor-element variations across the lamellae, although as expected a high correlation was observed between Fe and Mn. Although Van Kooten and Buseck (1978) observed fluctuations in Fe that could be correlated between compositional profiles in olivine grains, the Fe profile in the meteoritic grains is smooth, suggesting that controlling factors such as pressure variations proposed by Van Kooten and Buseck did not affect the meteoritic olivines.

On the basis of the few recognized examples of oscillatory zoning in olivine, there are several possible chemical associations. The trivalent ions might represent coupled substitutions of two trivalent ions into a tetrahedral site and either the M1 or M2 octahedral site, e.g., ($Al^{3+}$ + $Al^{3+}$), ($Al^{3+}$ + $Ti^{3+}$), etc. for ($Si^{4+}$ + $Mg^{2+}$). This substitution has been demonstrated experimentally where the solubility of spinel in forsterite reaches 0.5 mol% (Schlaudt and Roy, 1965). For the meteoritic forsterite, the elements normally present in the M sites (Ca, Mn, Fe, and Cr) would not show a measurable change in concentration because they are at low levels and the M substitutions would be mainly for Mg, for which small changes in a large concentration also could not be detected. Likewise, small changes in Si concentration normally could not be detected. Evidence, however, for Al substitution into the tetrahedral site of meteoritic forsterite was given by Steele (1986b) on the basis of an anticorrelation of Si and Al concentrations.

### Cause of oscillatory zoning

Most compositional studies on oscillatory zoning in mafic minerals have focused on pyroxene. Shimizu (1990) completed a detailed ion and electron probe study of augite from an alkaline basalt. Of the elements studied, he recognized two groups, incompatible and compatible, which approximately anticorrelate with each other. Thus, when a zone was found to be high in incompatible elements, including Ti, V, Zr, and Sr, the zone was depleted in compatible elements, including Cr and Sc. This relation does not appear to hold for the meteoritic olivine, for which the incompatible elements Ti and Al show oscillations, but at the same time the compatible elements Ca, Cr, and Fe show only monotonic changes. Shimizu (1990) concluded that this behavior in pyroxene was consistent with reaction-transport kinetics. In contrast, Downes (1974) described in detail the sector and oscillatory zoning in an augite phenocryst. In this case Ti and Al both correlated with the oscillations, but the major, compatible elements, including Mg, Fe, and Ca, showed only a monotonic change in the oscillatory zoned region. Downes (1974) considered that relative diffusion rates within the melt and crystal growth rates were important for forming oscillatory zoning in this augite. These chemical variations are very similar to that described above for the Allende forsterite.

The cause of oscillatory zoning as recognized in pyroxene and feldspar has been previously discussed (e.g., Haase et al., 1980; Allegre et al., 1981; Anderson, 1984; Ortoleva, 1990; Pearce and Kolisnik, 1990; Shimizu, 1990; L'Heureux and Fowler, 1994). It is generally agreed that there are several causes of zoning. Zoning caused by changes in macroscopic parameters such as pressure, influxes of new liquids, progressive changes in liquid composition, and cooling rate changes is thought to be reflected in coarse zoning features because the time scale of changes is long relative to the growth rate. Fine-scale oscillatory zoning in plagioclase has been attributed in one case to periodic relative motion of crystal and melt possibly because of tidal forces (Anderson, 1984). In contrast, other explanations of oscillatory zoning include an interaction near the crystal-liquid interface, where the composition of the liquid is controlled in part by the diffusion of components within the liquid, the rate of attachment (growth), and crystal-liquid partition coefficients. The scale of zoning changes in this case is considered to be on a scale of micrometers or tens of micrometers, and both mathematically (Allegre et al., 1981; L'Heureux and Fowler, 1994) and experimentally (Reeder et al., 1990) oscillatory zoning texturally similar to that described above for forsterite has been shown to result without any macroscopic change in the system.

A quantitative description of individual zoning patterns is complex because of many unknown or uncertain factors, such as diffusion coefficients for several elements in liquids of variable composition and distribution coefficients that are a function of bulk composition, temperature, individual element concentrations, and nonequilibrium growth kinetics at a poorly defined crystal surface. As a group, the trivalent ions all have a $Z^2R$($Z$ = ionic charge, $R$ = ionic radius) that results in slow diffusion relative to divalent ions in basalt (Hofmann, 1980). Some mathematical predictions can be made regarding the compositional profile of individual lamellae, which match those observed in the relatively simple plagioclase system (Allegre et al., 1981). Unfortunately, details of compositional profiles on a micrometer scale are very difficult to determine with the electron microprobe.

With such modeling as a guide, some general conclusions may be made regarding the conditions that existed during growth of oscillatory-zoned grains such as the forsterite in question. It is observed that oscillatory zoning is usually restricted to phenocrysts that have grown slowly relative to the surrounding matrix (Allegre et al., 1981). This and the fact that oscillatory zoning is rarely observed

in experimental systems (Lofgren, 1980) indicate that this type of zoning forms on the time scale of growth of phenocrysts in terrestrial or lunar lava flows. Likewise, Reeder et al. (1990) grew millimeter-size carbonate crystals showing oscillatory zoning in experiments lasting several days, a time similar to that expected for natural phenocryst growth from silicate melts. For plagioclase, Allegre et al. (1981) showed theoretically that oscillatory-zoned crystals must grow under conditions of very low supersaturation, i.e., in slow-growth conditions where nucleation is minimized and crystals grow to a relatively large size.

**Implications for origin of forsterite**

The source of forsterite in primitive meteorites is not known, but two proposals have been made. On the one hand, forsterite can be shown on the basis of thermodynamics to be a phase that could have condensed from the solar nebula under conditions thought to have existed, and there is mineralogical and geochemical evidence that some phases did form by this process (Grossman, 1972). These grains would then be incorporated into accreting meteorites. On the other hand, forsterite may grow from melts, and in particular chondrules have been proposed as a source of single grains of forsterite that are released after breakdown of the surrounding material of the chondrule (McSween, 1977).

Since these original proposals, other observations have been made and used as supporting evidence for the origin of forsterite. Minor elements have been determined in forsterite from many meteorites, and these data show unusual enrichments in refractory elements, including Al, Ca, Ti, V, and Sc (Steele, 1986a), all of which are thought to be characteristic of condensation processes. Jones (1992) has presented data showing that in one carbonaceous chondrite the isolated olivines are chemically equivalent to olivine grains found in chondrules of the same meteorite. Recently, Yoneda and Grossman (1994) made revised condensation calculations and showed that a melt phase can condense and coexist with other condensing phases, including forsterite. O isotopic measurements of single forsterite grains show enrichment in $^{16}O$ (Weinbruch et al., 1993; Hervig and Steele, 1992), which precludes crystallization from chondrules of known O composition. From these data there is no consensus on the origin of forsterite; indeed, more than one origin is possible. The discovery of oscillatory zoning as described here should provide additional evidence pointing to the source of some, if not all, forsterite.

Two occurrences of forsterite have been described that have similar major- and minor-element compositions, minor-element correlations, and spatial patterns of compositional variation. These two examples are from meteorites that belong to different meteorite classes. Although only two examples are described, about six other examples have been noted in both C3 and unequilibrated ordinary chondrites (UOC) meteorites. Because CL observation is not usually made under the conditions necessary to reveal the linear patterns described, the occurrence of oscillatory zoning is probably more common than these few examples indicate. Examples have not been seen in C2 meteorites, although luminescing forsterite is common. The similarity between forsterite in the C3 and UOC meteorites on the basis of minor-element variations has previously been recognized (Steele, 1986a); likewise, the difference between the forsterite in the C3 and UOC meteorites and that in C2 meteorites has been documented (Steele and Smith, 1986). The fine-scale spatial variation described in the present work reinforces the similarity between C3 and UOC forsterite.

The fact that forsterite with similar features occurs in two rather well-populated meteorite groups suggests that a common process created this material. Forsterite with these chemical and zoning features was also sufficiently widespread to be incorporated into meteorites that formed in different regions of the solar nebula, as suggested, for example, by differing bulk chemical (Wasson, 1985) and O isotopic compositions (Wasson, 1985) of the two meteorite classes. Oscillatory zoning is not observed in all forsterite grains either because it simply is not present or because the chemical variation is not sufficient to cause CL contrast. One can conclude that there is a range of forsterite, some of which shows oscillatory zoning and some of which doesn't, and any process that forms the forsterite must accommodate this variability.

For geologic samples that have clearly grown from a melt, oscillatory zoning has been commonly recognized in some crystals of feldspar and pyroxene and recently in olivine (Clark et al., 1986). For meteoritic forsterite, oscillatory zoning due to tidal fluctuations affecting a melt is not considered here because there is no evidence that appropriate conditions existed (tidal forces, magma body) during forsterite growth. This discussion focuses on the alternative boundary-layer effects. Mathematical considerations require that the diffusion of components adjacent to the growing crystal be sufficiently slow to create a concentration gradient, a condition that would occur in a liquid as opposed to a vapor. This implies that forsterite crystals showing oscillatory zoning grew from a melt rather than a vapor where concentration gradients would be difficult to maintain. Although vapor growth has been suggested as a possible growth mechanism for forsterite (Steele, 1986a), the presence of oscillatory zoning does not appear consistent, but this does not preclude the possibility of more than one growth mechanism.

By analogy with terrestrial lava flows, in which millimeter-size crystals of oscillatory-zoned plagioclase or pyroxene have grown, growth time would be on the order of days but would be a function of bulk composition and temperature, both of which control diffusion rates and are unknown. Growth of forsterite grains in chondrules requires that the cooling rates be similar to the slowest values derived from experimental studies that produce porphyritic chondrules (about 5 °C/h) (Hewins, 1983; Lofgren, 1989), both to achieve crystal sizes of several hundred micrometers and to form oscillatory zoning. Ex-

amples of oscillatory zoning in chondrule phases are rare, but such zoning does occur in orthopyroxene from a chondrule in Semarkona (Jones, 1993), where all measured elements, including Fe, Ca, Cr, Al, and Mn, vary with oscillations similar to those in the augite described by Shimizu (1990). A second example is of olivine in an enstatite chondrite where concentric zones from Fo3 to Fo75 are present (Lusby et al., 1987); no data were given for minor elements.

The presence of oscillatory zoning can be used as a possible criterion for recognizing the source material for isolated olivine grains because the source must also have olivine with similar zoning. Although the grain in 76004 is within an inclusion (possibly a chondrule), it is not clear that forsterite crystallized within this inclusion. The observation that the oscillatory zoning is truncated for this grain indicates a more complicated history than simple crystallization. It has been established that relict grains do occur within some chondrules (e.g., Steele, 1986a), which suggests that material was recycled during the chondrule-forming process. Although some chondrules may indeed contain forsterite that crystallized in situ with oscillatory zoning, none have been described other than the questionable ALHA 76004 grain recognized here. Jones (1992) described a match between the composition of forsterite found as single crystals and within the chondrules of the same meteorite (ALHA 77307); no CL observations were made, and it is not known whether any of these grains show oscillatory zoning.

Oscillatory zoning provides another test for the possible equivalence of forsterite grains. A systematic search should be made for chondrules containing forsterite with morphologies that indicate in situ crystallization and oscillatory zoning. It is possible that there exists no match for single crystals showing oscillatory zoning because the parental sample was disrupted and recycled completely. With the refined condensation calculations indicating that melt and crystals, including forsterite, can coexist (Yoneda and Grossman, 1994), the division between condensation and melt-crystal origin is less well defined, and it is therefore necessary to redefine possible mechanisms for the origin of meteoritic forsterite.

## Acknowledgments

Financial support was derived from NASA NAGW 3416 and 2272, and instrumental support was obtained through NSF EAR-9303530 and EAR-9316062. Critical reviews by Rhian Jones and Gary Lofgren provided comments that have helped to clarify both the presentation and interpretation of the data.

## References cited

Allegre, C.J., Provost, A., and Jaupart, C. (1981) Oscillatory zoning: A pathological case of crystal growth. Nature, 294, 223–228.

Anderson, A.T., Jr. (1984) Probable relations between plagioclase zoning and magma dynamics, Fuego Volcano, Guatemala. American Mineralogist, 69, 660–676.

Beckett, J.R., and Grossman, L. (1986) Oxygen fugacities in the solar nebula during crystallization of fassaite in Allende inclusions (abs.). Lunar and Planetary Science, XVII, 36–37.

Beckett, J.R., Live, D., Tsay, F-D., Grossman, L., and Stolper, E. (1988) $Ti^{3+}$ in meteoritic and synthetic hibonite. Geochimica et Cosmochimica Acta, 52, 1479–1495.

Burns, R.G., Vaughn, D.J., Abu-Eid, R.M., and Witner, M. (1973) Spectral evidence for $Cr^{3+}$, $Ti^{3+}$, and $Fe^{2+}$ rather than $Cr^{2+}$, and $Fe^{3+}$ in lunar ferromagnesian silicates. Proceedings of the Fourth Lunar Science Conference, 983–994.

Clark, A.H., Pearce, T.H., Roeder, P.L., and Wolfson, I. (1986) Oscillatory zoning and other microstructures in magmatic olivine and augite: Nomarski interference contrast observations on etched polished surfaces. American Mineralogist, 71, 734–741.

Downes, M.J. (1974) Sector and oscillatory zoning in calcic augites from M. Etna, Sicily. Contributions to Mineralogy and Petrology, 47, 187–196.

Gonzalez, R.C., and Wintz, P. (1987) Digital image processing, 503 p. Addison-Wesley, Reading, Massachusetts.

Grossman, L. (1972) Condensation in the primitive solar nebula. Geochimica et Cosmochimica Acta, 36, 597–617.

Haase, C.S., Chadam, J., Feinn, D., and Ortoleva, P. (1980) Oscillatory zoning in plagioclase feldspar. Science, 209, 272–274.

Hervig, R.L., and Steele, I.M. (1992) Oxygen isotopic analysis of Allende olivine by ion microprobe and implication for chondrule origin (abs.). Lunar and Planetary Science, XXIII, 525–526.

Hewins, R.H. (1983) Dynamic crystallization experiments as constraints on chondrule genesis. In E.A. King, Ed., Chondrules and their origins, p. 122–133. Lunar and Planetary Institute, Houston, Texas.

Hofmann, A.W. (1980) Diffusion in natural silicate melts: A critical review. In R.B. Hargraves, Ed., Physics of magmatic processes, p. 385–417. Princeton University Press, Princeton, New Jersey.

Ito, J. (1977) Crystal synthesis of a new olivine, $LiScSiO_4$. American Mineralogist, 62, 356–361.

Jones, R.H. (1992) On the relationship between isolated and chondrule olivine grains in the carbonaceous chondrite ALHA 77307. Geochimica et Cosmochimica Acta, 56, 467–482.

——— (1993) Complex zoning behavior in pyroxene in FeO-rich chondrules in the Semarkona ordinary chondrite (abs.). Lunar and Planetary Science, XXIV, 735–736.

L'Heureux, I., and Fowler, A.D. (1994) A nonlinear dynamical model of oscillatory zoning in plagioclase. American Mineralogist, 79, 885–891.

Lofgren, G. (1980) Experimental studies on the dynamic crystallization of silicate melts. In R.B. Hargraves, Ed., Physics of magmatic processes, p. 487–551. Princeton University Press, Princeton, New Jersey.

——— (1989) Dynamic crystallization of chondrule melts of porphyritic olivine composition: Textures experimental and natural. Geochimica et Cosmochimica Acta, 53, 461–470.

Lusby, D., Scott, E.R.D., and Keil, K. (1987) Ubiquitous high-FeO silicates in enstatite chondrites. Proceedings of the Seventeenth Lunar and Planetary Science Conference. Journal of Geophysical Research, 92, E679–E695.

Mayeda, T.K., Clayton, R.N., and Olsen, E.J. (1980) Oxygen isotope anomalies in an ordinary chondrite. Meteoritics, 15, 330–331.

McSween, H.Y. (1977) On the nature and origin of isolated olivine grains in carbonaceous chondrites. Geochimica et Cosmochimica Acta, 41, 411–418.

Olsen, E., and Grossman, L. (1978) On the origin of isolated olivine grains in type 2 carbonaceous chondrites. Earth and Planetary Science Letters, 41, 111–127.

Olsen, E., Noonan, A., Fredriksson, K., Jarosewich, E., and Moreland, G. (1978) Eleven new meteorites from Antarctica, 1967–1977. Meteoritics, 13, 209–225.

Ortoleva, P.J. (1990) Role of attachment kinetic feedback in the oscillatory zoning of crystals grown from melts. Earth-Science Reviews, 29, 3–8.

Pearce, T.H., and Kolisnik, A.M. (1990) Observations of plagioclase zoning using interference imaging. Earth-Science Reviews, 29, 9–26.

Petaev, M.I., and Brearley, A.J. (1994) Exsolution in ferromagnesian olivine of the Divnoe meteorite. Science, 266, 1545–1547.

Reeder, R.J., Fagioli, R.O., and Myers, W.J. (1990) Oscillatory zoning of Mn in solution-grown calcite crystals. Earth-Science Reviews, 29, 39–46.

Scheetz, B.E., and White, W.B. (1972) Synthesis and optical absorption

spectra of $Cr^{2+}$-containing orthosilicates. Contributions to Mineralogy and Petrology, 37, 221–227.

Schlaudt, C.M., and Roy, D.M. (1965) Crystalline solution in the system $MgO$-$Mg_2SiO_4$-$MgAl_2O_4$. Journal of the American Ceramic Society, 48, 248–251.

Shimizu, N. (1990) The oscillatory trace element zoning of augite phenocrysts. Earth-Science Reviews, 29, 27–37.

Steele, I.M. (1986a) Compositions and textures of relic forsterite in carbonaceous and unequilibrated ordinary chondrites. Geochimica et Cosmochimica Acta, 50, 1379–1396.

——— (1986b) Cathodoluminescence and minor elements in forsterites from extraterrestrial samples. American Mineralogist, 71, 966–970.

——— (1989) Compositions of isolated forsterites in Ornans (C3O). Geochimica et Cosmochimica Acta, 53, 2069–2080.

——— (1990) Micro-textural and -chemical features of isolated forsterites of C3 meteorites with implications for origin (abs.). Lunar and Planetary Science, XXI, 1196–1197.

——— (1992) Digitized cathodoluminescence imaging of minerals. Scanning Microscopy, 5, 611–618.

Steele, I.M., and Smith, J.V. (1986) Contrasting forsterite compositions for C2, C3, and UOC meteorites; evidence for divergence from common parent (abs.). Lunar and Planetary Science, XV, 822–823.

Steele, I.M., Smith, J.V., and Skirius, C. (1985) Cathodoluminescence, minor elements and zoning in forsterites from Murchison (C2) and Allende (C3V) carbonaceous chondrites. Nature, 313, 294–297.

Sutton, S.R., Jones, K.W., Gordon, B., Rivers, M.L., Bajt, S., and Smith, J.V. (1993) Reduced chromium in olivine grains from lunar basalt 15555: X-ray absorption near edge structure (XANES). Geochimica et Cosmochimica Acta, 57, 461–468.

Van Kooten, G.K., and Buseck, P.R. (1978) Interpretation of olivine zoning: Study of a maar from the San Francisco volcanic field, Arizona. Geological Society of America Bulletin, 89, 744–754.

Wasson, J.T. (1985) Meteorites: Their record of early solar-system history, 267 p. Freeman, New York.

Watson, E.B. (1979) Calcium content of forsterite coexisting with silicate liquid in the system $Na_2O$-$CaO$-$MgO$-$Al_2O_3$-$SiO_2$. American Mineralogist, 64, 824–829.

Weinbruch, S., Zinner, E.K., El Goresy, A., Steele, I.M., and Palme, H. (1993) Oxygen isotopic composition of individual olivine grains from the Allende meteorite. Geochimica et Cosmochimica Acta, 57, 2649–2661.

Yoneda, S., and Grossman, L. (1994) Calculated stability field and compositions of nonideal condensate liquids in a solar gas (abs.). Meteoritics, 29, 554–555.

MANUSCRIPT RECEIVED MAY 13, 1994
MANUSCRIPT ACCEPTED APRIL 13, 1995